SPECIAL TOPIC — Acoustics

Bearing splitting and near-surface source ranging in the direct zone of deep water*

Jun-Nan Wu(吴俊楠)[1,2], Shi-Hong Zhou(周士弘)[1,†], Zhao-Hui Peng(彭朝晖)[1], Yan Zhang(张岩)[1], and Ren-He Zhang(张仁和)[1]

[1] *State Key Laboratory of Acoustics, Institute of Acoustics, Chinese Academy of Sciences, Beijing* 100190, *China*

[2] *College of Physics, University of Chinese Academy of Sciences, Beijing* 100049, *China*

(Received 1 May 2016; revised manuscript received 1 Sepember 2016; published online 25 October 2016)

Sound multipath propagation is very important for target localization and identification in different acoustical zones of deep water. In order to distinguish the multipath characteristics in deep water, the Northwest Pacific Acoustic Experiment was conducted in 2015. A low-frequency horizontal line array towed at the depth of around 150 m on a receiving ship was used to receive the noise radiated by the source ship. During this experiment, a bearing-splitting phenomenon in the direct zone was observed through conventional beamforming of the horizontal line array within the frequency band 160 Hz–360 Hz. In this paper, this phenomenon is explained based on ray theory. In principle, the received signal in the direct zone of deep water arrives from two general paths including a direct one and bottom bounced one, which vary considerably in arrival angles. The split bearings correspond to the contributions of these two paths. The bearing-splitting phenomenon is demonstrated by numerical simulations of the bearing-time records and experimental results, and they are well consistent with each other. Then a near-surface source ranging approach based on the arrival angles of direct path and bottom bounced path in the direct zone is presented as an application of bearing splitting and is verified by experimental results. Finally, the applicability of the proposed ranging approach for an underwater source within several hundred meters in depth in the direct zone is also analyzed and demonstrated by simulations.

Keywords: direct zone, deep water, bearing splitting, near-surface source ranging

PACS: 43.30.Cq, 43.60.Fg, 43.60.Jn **DOI:** 10.1088/1674-1056/25/12/124311

1. Introduction

In the typical deep ocean, there generally exist the sound propagations of direct zone, shadow zones, and convergence zones for shallow source/receiver pairs. The range of direct zone (DZ) is always close, covering about several kilometers due to the water refraction depending on the gradient of the near-surface sound speed profile (SSP) and the source/receiver depths. In DZ, sound signals arrive at the receiver through direct and surface-reflected ray path propagation with small arrival angles (or launching angles) of several degrees. For low-frequency sound signals with less reflection loss than that for the high-frequency signals, bottom-reflected ray paths in DZ should also be taken into account, which arrive at the receiver with very large arrival angles. The sound field in shadow zones primarily comes from bottom-reflected ray paths with range-dependent arrival angles. The water-refracted ray paths far from the source interfere constructively without bottom interaction and contribute to the strong sound field in convergence zones. It is very important to understand the sound field for underwater acoustic applications in deep water.

In 2015, the Northwest Pacific Acoustic Experiment was conducted by the State Key Laboratory of Acoustics, Institute of Acoustics, Chinese Academy of Sciences. Passing of a source ship and a tow ship was involved during the experiment. The noise signals radiated from the source ship and were recorded on a low-frequency horizontal line array (HLA) towed by the receiving ship. During this experiment, broadband towed HLA measurements from the shadow zone to the closest point of approach (CPA) of two passing ships (source/receiver) were performed. A source bearing-splitting phenomenon in the direct zone was observed through low-frequency HLA's conventional beamforming (CBF). In principle, the low-frequency sound field in the DZ of deep water is mainly contributed by direct-path (DP) rays (including surface reflected ones) and bottom bounced (BB) rays. There exists a very distinct difference between DP rays and BB rays in arrival angles, which causes source bearing splitting in DZ. The phenomenon was also observed in the North Pacific Acoustic Laboratory Philippine Sea 2009 experiment.[1] In Ref. [1], Heaney *et al.* analyzed the experimental data and focused on the variance of bottom bounce energy due to the scattering effects of rough seafloor and sea surface. Actually, beam-spreading of HLA is common in the underwater waveguide due to multipath propagation, which degrades the resolution

*Project supported by the Program of One Hundred Talented People of the Chinese Academy of Sciences and the National Natural Science Foundation of China (Grant Nos. 11434012 and 41561144006).

†Corresponding author. E-mail: shih_zhou@mail.ioa.ac.cn

© 2016 Chinese Physical Society and IOP Publishing Ltd

and array gain of the formed beams, especially in the endfire direction of the array. Buckingham[2] presented a theoretical analysis of the response of a towed array to the acoustic field in isovelocity shallow water, revealing that when the source is endfire-on to the array, beam broadening or, in the extreme cases, beam splitting due to a different angular response to each of the modes may exist. Yang[3] indicated that for a near endfire source in shallow water, signal-arrival angles were associated with different modes. Each mode led to its own bearing and thus beam broadened. Ma *et al.*[4] gave the simulated CBF results of the tow ship's noise. The results showed that the maximum output of the towed line array was widely spread and away from the endfire as a result of near-field multipath propagation, which influenced strongly the target detection near the endfire of the horizontal array. However, serious bearing-splitting is less common due to a little difference of multipath arrival angles.

Source ranging has always been a hot topic in underwater acoustics, and a variety of approaches have been developed.[5–7] One of the most common methods is based on time delay of multiple paths. Evan and David[8] made a source track localization via cross correlating the received signals at horizontally separated receivers and matching the measured and simulated correlation time delay in shallow water. Duan *et al.*[9] localized a moving source by tracking the time delay of the direct and surface-reflected arrivals in the reliable acoustic path in deep water. Wu *et al.*[10] achieved the near-surface source ranging by extracting time delay between bottom-reflected and bottom-surface-reflected arrivals from the interference pattern of sound intensity in frequency and time domain in the first shadow zone of deep water. For a shallow source–receiver pair in DZ, however, a time delay of several seconds between DP path and BB path can hardly be extracted in practical applications. Moreover, the amplitudes of the two paths differ evidently and their correlation coefficient is too small to be identified. In this paper, a near-surface source ranging approach is presented by avoiding the calculation of time delay and taking full advantage of the split bearings of DP and BB paths in DZ. The approach is demonstrated by experimental data. As an extension, the applicability of the proposed approach in DZ for an underwater source within several hundred meters deep is also analyzed and demonstrated by simulations.

The rest of this paper is organized as follows. In Section 2, the Northwest Pacific Acoustic Experiment is briefly reviewed, and the bearing splitting in DZ through the broadband CBF is presented. In Section 3, the bearing-splitting phenomenon is explained by using ray theory and comparing the simulated CBF results with experimental ones. Near-surface source ranging based on the split bearings in DZ is analyzed in Section 4, and the applicability of the proposed approach is analyzed in Section 5. A summary is presented in Section 6.

2. Experimental review and signal measurements

In 2015, an acoustic experiment was done in the Northwest Pacific, with a towed HLA deployed on the receiving ship with a towed depth of around 150 m. The voyage speed was 4 knots. During the experiment, a source ship with a draft of around 6 m sailed close to the receiving ship, passed across the DZ, and then moved away. The array recorded the noise radiated from the source ship. The water depth was about 5200 m. The GPS positions, distances and relative bearings of the receiving ship and source ship during the passing period are shown in Fig. 1. Figure 1(a) shows the GPS positions during the experiment. Figures 1(b) and 1(c) show the source–receiver distances and their relative bearings, respectively. The CPA was at about 29 min and the closest distance was about 2 km.

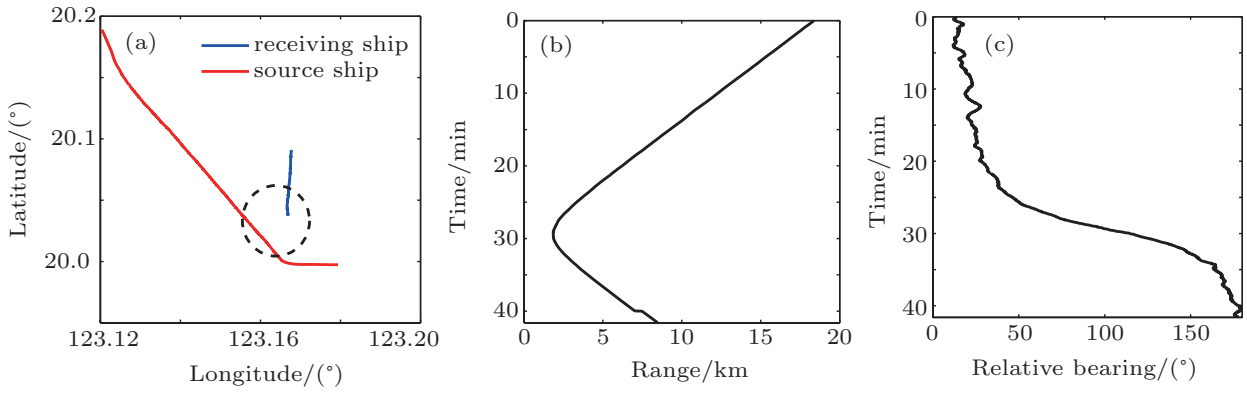


Fig. 1. (color online) (a) Source and receiving ship's GPS positions during the experiment. The black circle is the schematic DZ of the receiving ship. (b) Source–receiver distances. (c) Relative bearings.

Figure 2 shows the bearing-time record (BTR) calculated by the broadband (160 Hz–360 Hz) CBF during the crossing. It includes closing from a range of 18 km, the CPA and moving away. The black line represents the true source bearing. The strong energy at 10° near the endfire comes from the noise radiated by the tow ship, which is similar to that in shallow water.[4] From Fig. 2, an interesting and important phenomenon can be seen that the source's bearing splits into two

different parts from 25 min to 34 min. One is close to the real bearing and has a higher bearing-rate and less beam-spreading, corresponding to the direct path. The other is deviated from the real bearing and has a lower bearing-rate and strong beam-spreading, which comes from the BB path propagation and extends to the shadow zone outside the time window 25 min–34 min. The bearing deviation in the shadow zone has been discussed in Ref. [11].

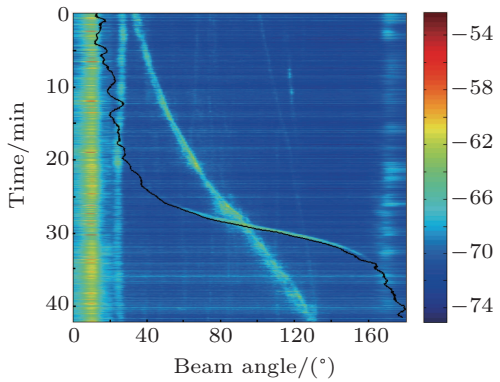


Fig. 2. (color online) Bearing time record during the crossing. The black line represents the true source bearing.

The cross bearing-time record in Fig. 2 actually shows the same target ship. It is easy to be misjudged as two different targets. This paper focuses on explaining this bearing-splitting phenomenon in DZ theoretically and numerically, and then applying it for the near-surface source ranging.

3. Theoretical analysis and simulation results

In terms of ray theory, a formal solution of the acoustic wave equation in a range-independent environment can be obtained from the transport equation and the eikonal equation.[12] The solution of the sound pressure field to the wave equation for a receiver at range r and depth z follows the form

$$p(r,z,\omega)=\sum_{m=1}^{M}A_m(r,z,\omega)\,\mathrm{e}^{\mathrm{j}k_{\mathrm{s}}\varphi_m(r,z)}, \tag{1}$$

where M is the total number of eigenrays, A_m and φ_m are the pressure amplitude and eikonal for the m-th eigenray, respectively, and $k_{\mathrm{s}}=\omega/c_{\mathrm{s}}$ is the wavenumber with c_{s} being the sound speed at the source position.

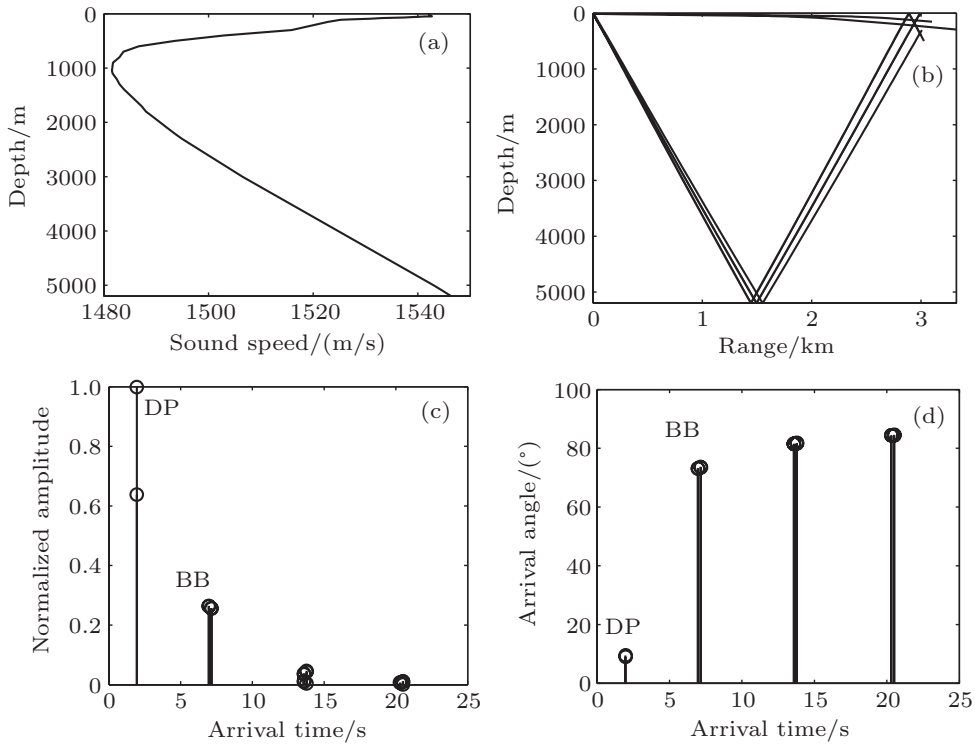


Fig. 3. Eigenrays' arrival structure at the 3-km range for the shallow source and receiver pair in the direct zone. (a) Measured SSP from the Northwest Pacific. (b) Eigenrays. (c) Normalized amplitude. (d) Arrival angles.

By solving the eikonal equation, we can obtain the eikonal[13]

$$\varphi_m(r,z)=r\cos\alpha_{sm}+\int\sqrt{n^2(z)-\cos^2\alpha_{sm}}\,\mathrm{d}z, \tag{2}$$

where $n(z)=c_{\mathrm{s}}/c(z)$ is the refractive index, and α_{sm} is the launching angle of the ray with respect to the horizontal. Substituting Eq. (2) into Eq. (1) and applying Snell's law, the sound pressure can be written as

$$\begin{aligned}p(r,z,\omega)&=\sum_{m=1}^{M}A_m(r,z,\omega)\exp\left(\mathrm{j}k_{\mathrm{s}}\left[r\cos\alpha_{sm}\right.\right.\\&\quad\left.\left.+\int\sqrt{n^2(z)-\cos^2\alpha_{sm}}\,\mathrm{d}z\right]\right)\\&=\sum_{m=1}^{M}Q_m(r,z,\omega)\,\mathrm{e}^{\mathrm{j}k_0r\cos\alpha_{0m}},\end{aligned} \tag{3}$$

where $k_0 = \omega/c_0$ with c_0 being the sound speed at the receiver, and α_{0m} is the arrival angle with respect to the horizontal. $Q_m(r,z,\omega) = A_m(r,z,\omega)\exp(\mathrm{j}k_s \int \sqrt{n^2(z) - \cos^2\alpha_{sm}}\,\mathrm{d}z)$, which is correlated with the m-th eigenray. Its phase is independent of range.

Eigenrays' arrival structure from a 6-m deep source to a 150-m deep receiver located 3 km away, calculated by the Bellhop program[14] is shown in Fig. 3.[14] Figure 3(a) shows the measured SSP from the at-sea Northwest Pacific experiment with a 50-m-deep surface channel. Figure 3(b) shows the eigenrays including the DP and BB paths. As shown intuitively in Fig. 3(c), the DZ sound field is mostly contributed by DP and BB paths. Other paths with twice or more bottom bounces can be neglected due to serious sound attenuation. Figure 3(d) shows the arrival angles versus arrival time of DP and BB paths. It shows that arrival angles of DP are around 10°, while those of BB path are more than 70°.

For the direct sound field, equation (3) can be simplified into the summation of DP and BB paths:

$$p(r,z,\omega) = \mathrm{e}^{\mathrm{j}k_0 r\cos\alpha_{01}} \sum_{m=1}^{M_1} Q_m(r,z,\omega) + \mathrm{e}^{\mathrm{j}k_0 r\cos\alpha_{02}} \sum_{m=1}^{M_2} Q'_m(r,z,\omega), \tag{4}$$

where α_{01} and M_1 are the arrival angle and number of DP ray paths, respectively. Likewise, α_{02} and M_2 are the arrival angle and number of BB ray paths, respectively.

Then we analyze the conventional beamforming outputs of a towed horizontal line array. Again, we employ a ray representation of the direct sound field

$$p_n(r_n,z,\omega) = \mathrm{e}^{\mathrm{j}k_0 r_n\cos\alpha_{01}} \sum_{m=1}^{M_1} Q_m(r_n,z,\omega) + \mathrm{e}^{\mathrm{j}k_0 r_n\cos\alpha_{02}} \sum_{m=1}^{M_2} Q'_m(r_n,z,\omega), \tag{5}$$

where r_n is the range from the source to the n-th element, and all elements are at the same depth z. Assuming an array of N uniformly spaced elements, with spacing d in between, the conventional beamforming outputs are obtained by

$$B(\theta,\omega) = \left| \sum_{n=1}^{N} p_n(r_n,z,\omega)\,\mathrm{e}^{\mathrm{j}k_0(n-1)d\cos\theta} \right|^2, \tag{6}$$

where angle θ is measured from the endfire of the array. For the analytical calculations, a far field approximation of the source–receiver range is taken as

$$r_n \approx r_0 - (n-1)d\cos\theta_{\mathrm{T}}, \tag{7}$$

where r_0 is the range to the first element of the array and θ_{T} is the real target bearing. Substituting Eqs. (5) and (7) into Eq. (6), the beam intensity spectrum in the DZ can be written as

$$B(\theta,\omega) = \left| \sum_{n=1}^{N} \left[\begin{array}{l} \displaystyle\sum_{m=1}^{M_1} Q_m(r_n,z,\omega)\,\mathrm{e}^{\mathrm{j}k_0 r_0\cos\alpha_{01}} \exp(\mathrm{j}k_0(n-1)d(\cos\theta - \cos\alpha_{01}\cos\theta_{\mathrm{T}})) \\ \displaystyle + \sum_{m=1}^{M_2} Q'_m(r_n,z,\omega)\,\mathrm{e}^{\mathrm{j}k_0 r_0\cos\alpha_{02}} \exp(\mathrm{j}k_0(n-1)d(\cos\theta - \cos\alpha_{02}\cos\theta_{\mathrm{T}})) \end{array} \right] \right|^2, \tag{8}$$

which shows that the beam intensity is contributed by arrivals of DP and BB paths. Note the following:

(i) when the source is in the broadside direction, $\cos\theta_{\mathrm{T}} = 0$, both groups of arrivals appear in one beam with $\theta = \theta_{\mathrm{T}} = 90°$, so there will be neither bearing splitting nor bearing deviation;

(ii) for a nonbroadside source, $\cos\theta_{\mathrm{T}} \neq 0$, the arrivals split into two beams with the angles determined by

$$\cos\theta_1 = \cos\alpha_{01}\cos\theta_{\mathrm{T}}, \quad \cos\theta_2 = \cos\alpha_{02}\cos\theta_{\mathrm{T}}. \tag{9}$$

Thus, there will be two estimated bearings in the beam pattern, and the beam angles are closely related to target bearing and the arrival angles of DP or BB rays. Figure 4 presents the arrival angles of DP and BB paths from a 6-m deep source to a 150-m deep receiver at a range of 1 km–10 km. It can be seen that the width of DZ is 4 km, and the arrival angles are around 10° for DP and more than 70° for the BB path, respectively. In general, for shallow source/receiver pairs in the DZ of deep water, the arrival angles of DP are usually small, $\cos\alpha_{01} \approx 1$, and therefore the estimated bearing $\theta_1 \approx \theta_{\mathrm{T}}$. On the other hand, arrival angles of BB paths are very large, and as a result, the estimated bearing θ_2 will be deviated from θ_{T} to the broadside direction by many degrees. Combining Eq. (9), it can be seen that for a certain source–receiver range with a certain arrival angle, the closer to the endfire direction the target, the greater the deviation between estimated bearing and the real one is. For a certain target bearing, the further the range, the smaller the deviation is. It can also be seen from Fig. 4 that the arrival angles of DP change slowly with range, while those of BB paths decrease monotonically with increasing range, which will be used for range estimation in the following section.

(iii) As for the endfire case, θ_1 is also offset from θ_{T} and spreads a lot. This is similar to the phenomenon in shallow water, which has been explained by Yang.[3]

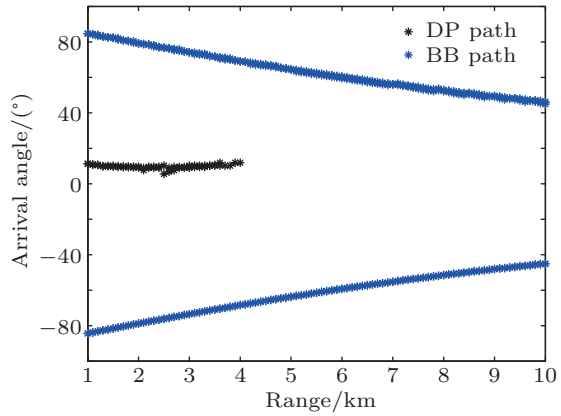


Fig. 4. (color online) Arrival angles of DP and BB paths for a source within a range of 10 km.

For numerical simulations of the beam pattern, we shall use the same acoustic environment as that shown in Fig. 3(a). The bottom is a flat homogeneous half-space with sound speed 1600 m/s, the density 1.6 g/cm^3 and the attenuation coefficient 0.2 dB/λ. The source is 6-m deep, while the HLA receiver is 150-m deep, with 160 elements in which the spacing between two elements is 2 m. Simulated results of BTR by the broadband (160 Hz–360 Hz) CBF are shown in Fig. 5, and for comparison, the same ranges and bearings (shown as the black dotted line) as experimental data are used.

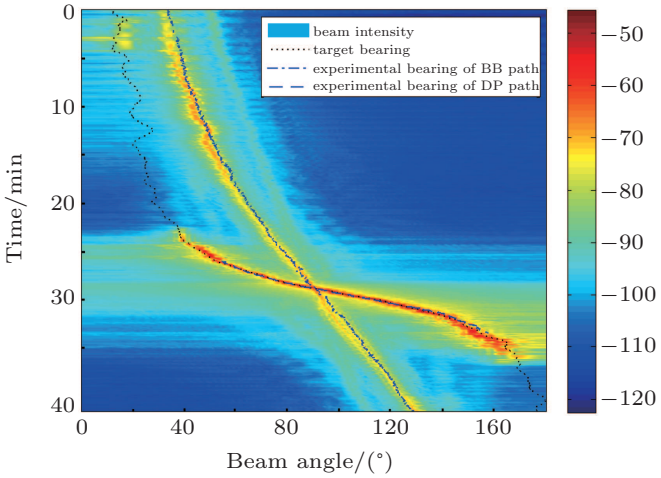


Fig. 5. (color online) Simulated BTR results by using the same ranges and bearings as experimental data. Black dotted line: Target bearing. Blue dot dashed line: experimental bearing of BB path. Blue dash line: experimental bearing of DP.

It can be seen that in DZ, BTR is classified into two groups as predicted by the theoretical analysis. The first one corresponds to DP, which has a higher bearing rate, peaks at CPA, and approaches to the real bearing. This group of energy falls off with range as the source moves out of the direct zone. The second one arrives within the whole time. It has a lower bearing rate, and is closer to the broadside. This group corresponds to BB paths. Experimental bearings of DP (blue dashed line) and BB paths (blue dot dashed line) extracted from Fig. 2 are also indicated in Fig. 5. They are similar to the simulated bearings.

4. Application to near-surface source ranging

Based on the split bearings, near-surface source ranges can be estimated in DZ. By using the ray theory, the relationship between range and depth can be described as[13]

$$\mathrm{d}r = |\cot\alpha(z)|\,\mathrm{d}z, \tag{10}$$

where $\alpha(z)$ is the grazing angle of the ray at depth z with respect to the horizontal direction. Considering the arrival angle of the BB path and integrating Eq. (10) as shown in Fig. 6 schematically, the range can be written as

$$\begin{aligned} r &= \int_{z_\mathrm{s}}^{H}\left|\frac{\cos\alpha(z)}{\sin\alpha(z)}\right|\mathrm{d}z+\int_{z_\mathrm{r}}^{H}\left|\frac{\cos\alpha(z)}{\sin\alpha(z)}\right|\mathrm{d}z \\ &= \int_{z_\mathrm{s}}^{H}\frac{1}{\sqrt{\dfrac{1}{\cos^2\alpha(z)}-1}}\mathrm{d}z+\int_{z_\mathrm{r}}^{H}\frac{1}{\sqrt{\dfrac{1}{\cos^2\alpha(z)}-1}}\mathrm{d}z \\ &= \int_{z_\mathrm{s}}^{H}\frac{c(z)}{\sqrt{\left(\dfrac{c(z)}{\cos\alpha(z)}\right)^2-c^2(z)}}\mathrm{d}z \\ &\quad+\int_{z_\mathrm{r}}^{H}\frac{c(z)}{\sqrt{\left(\dfrac{c(z)}{\cos\alpha(z)}\right)^2-c^2(z)}}\mathrm{d}z, \end{aligned} \tag{11}$$

where H, z_s, and z_r are the water depth, source depth and receiver depth, respectively.

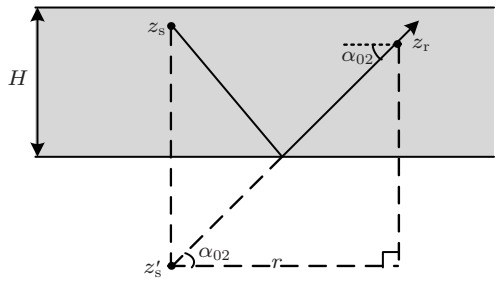


Fig. 6. Schematic diagram of BB path simplified in a straight line.

Applying Snell's Law, equation (11) can be transformed into

$$\begin{aligned} r &= \int_{z_\mathrm{s}}^{H}\frac{c(z)}{\sqrt{\left(\dfrac{c_0}{\cos\alpha_{02}}\right)^2-c^2(z)}}\mathrm{d}z \\ &\quad+\int_{z_\mathrm{r}}^{H}\frac{c(z)}{\sqrt{\left(\dfrac{c_0}{\cos\alpha_{02}}\right)^2-c^2(z)}}\mathrm{d}z. \end{aligned} \tag{12}$$

As can be seen in Eq. (12), the source–receiver range is related to SSP, water depth, source/receiver depths and arrival angle α_{02} of BB ray paths. Usually, SSP and water depth can be measured, and HLA depth is known. Thus the range is correlated with source depth and arrival angle. For a near-surface source, the depth can be considered to be about 6 m. Then the range is only dependent on the arrival angle of the BB path.

Recalling the analysis in Section 3, the bearing of DP is approximately equal to the real target bearing. Then the bearing of the BB path in Eq. (9) can be written as

$$\cos\theta_2 = \cos\alpha_{02}\cos\theta_T \approx \cos\alpha_{02}\cos\theta_1, \tag{13}$$

yielding

$$\cos\alpha_{02} \approx \frac{\cos\theta_2}{\cos\theta_1}. \tag{14}$$

Equation (14) indicates that the arrival angle of the BB path can be estimated by the split bearings θ_1 and θ_2. Note that equation (14) is unsuitable for the broadside case as the denominator cannot be zero. To handle this, the differential operation on both sides of Eq. (13), i.e.

$$\sin\theta_2\,\mathrm{d}\theta_2 \approx \cos\alpha_{02}\sin\theta_1\,\mathrm{d}\theta_1 \tag{15}$$

yields

$$\cos\alpha_{02} \approx \frac{\sin\theta_2\,\mathrm{d}\theta_2}{\sin\theta_1\,\mathrm{d}\theta_1}. \tag{16}$$

Equation (16) is only suitable for the near-broadside case as the arrival angle here changes slowly.

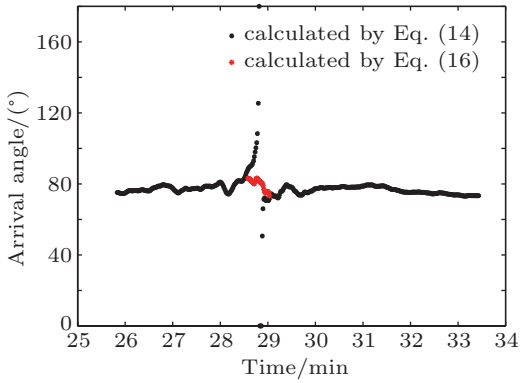


Fig. 7. (color online) Arrival angles calculated by Eq. (14) and Eq. (16), respectively.

Now we apply this method to the experimental data which have been analyzed in Section 2. Before calculating the arrival angles, the preprocessing of sliding linear fitting for the experimental estimated bearings every 10 s is needed in order to reduce the bearing fluctuation. Then the arrival angles are estimated and plotted in Fig. 7. The black dots indicate α_{02} calculated by Eq. (14), which is abnormal near the broadside of HLA. The red stars within 5° of the broadside indicate α_{02} calculated by Eq. (16). Then the arrival angles along with time could be modified by replacing the abnormal points with the red stars. Substituting the arrival angles into Eq. (12), source–receiver ranges could be obtained. Figure 8 shows the estimated ranges and the real ranges (black line) as the source ship passes across DZ of the receiver. It can be seen that the estimated ranges fit well with the real one. The error near the broadside is larger than the others: the error comes from an estimation error of arrival angle α_{02}. As the beam with respect to the BB path is broadened, the errors of extracted bearings from BTR are inevitable.

Taking the differential on both sides of Eq. (14) yields

$$\sin\alpha_{02}\,\mathrm{d}\alpha_{02} \approx \frac{\cos\theta_2\sin\theta_1}{\cos^2\theta_1}\,\mathrm{d}\theta_1 + \frac{\sin\theta_2}{\cos\theta_1}\,\mathrm{d}\theta_2. \tag{17}$$

When the source is near the broadside, α_{02}, θ_1, and θ_2 are all close to 90°. Then from Eq. (17), it can be seen that the nearer to the broadside the source, the larger the estimation error of arrival angle α_{02} is. Even so, the errors are still acceptable for practical applications.

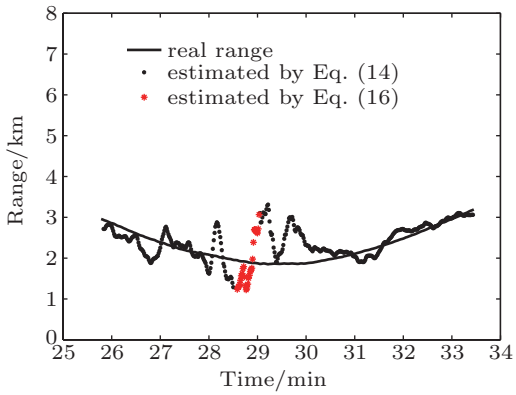


Fig. 8. (color online) Ranges estimated by the split bearings.

5. Applicability analysis for underwater source ranging

During the above analysis, source depth is assumed to be a surface source (set to be 6-m deep). In practice, however, it is necessary to discuss the applicability of Eq. (12) for an underwater source (with unknown depth) when the BB path of the sound field is strong enough to be detected. In this section, the performance of the ranging approach for an underwater source within 300-m deep is analyzed. For convenience of analysis, it is reasonable to simplify the BB path into a straight line, shown in Fig. 6 schematically. Through the geometric relationship in Fig. 6, we have

$$\tan\alpha_{02} = \frac{2H - z_s - z_r}{r}. \tag{18}$$

Then taking the differential of Eq. (18) yields

$$\mathrm{d}\alpha_{02} = -\frac{\cos^2\alpha_{02}}{r}\,\mathrm{d}z_s, \tag{19}$$

$$\mathrm{d}r = -\frac{1}{\tan\alpha_{02}}\,\mathrm{d}z_s. \tag{20}$$

Equation (19) shows that arrival angle α_{02} of the BB path decreases with increasing source depth z_s. Generally, with α_{02} being more than 70° and r on the order of 10^3 m, α_{02} varies slightly when $\mathrm{d}z_s$ is within several hundred meters. Figure 9 gives the arrival angles at different source depths for a receiver depth of 150 m located 3 km away. It shows that for all source depths from 10 m to 300 m, the arrival angles of DP are small, while those of the BB path are large and fluctuate less than 1°.

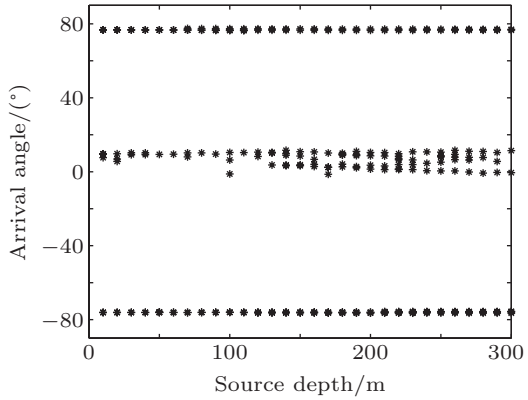


Fig. 9. Arrival angles at different source depths for a receiver depth of 150 m located 3 km away.

From Eq. (20), assuming that $\alpha_{02} = 70°$, $\mathrm{d}z_s = 300$ m, then $\mathrm{d}r = 109$ m. It means that the estimation error of the range is theoretically less than 109 m for an underwater source within 300 m in depth, which is acceptable in practical application.

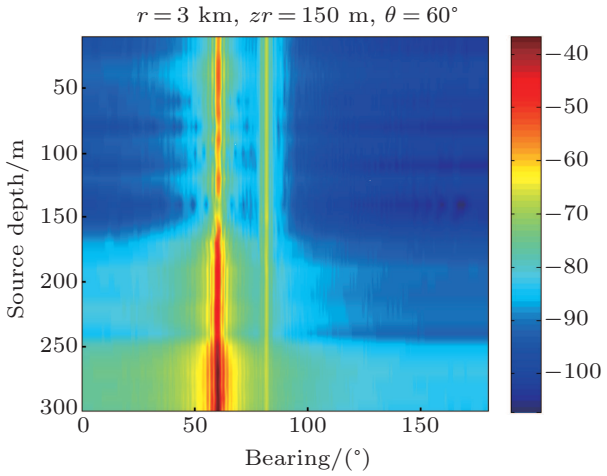


Fig. 10. (color online) Beam output of HLA at 150 m in depth with a source bearing of 60° located 3 km away.

In the following simulations, we consider the source range estimation with the source depth changing from 10 m to 300 m. The source–receiver range is 3 km, HLA depth is 150 m, and the target bearing is 60 °. By conventional beamforming, the beam intensity output with a 0.1° sampling interval is shown in Fig. 10. It shows that the detected bearings corresponding to the DP beam and BB beam are weakly dependent on source depth. Extracting the two bearings, arrival angles can be estimated by Eq. (14). Then the source range can be estimated by substituting them into Eq. (12). Figure 11(a) gives the estimated range, where red circles indicate the ranges estimated with a supposed source depth of 6 m, which means the depth of a near-surface source. The relative estimation error is shown in Fig. 11(b). It reveals that when taking an underwater source as a near-surface source, the estimated range values are larger than the real values with an average error of less than 3%. It means that equation (12) is also suitable for estimating the range of underwater source within a several hundred meters's depth in DZ if the underwater source depth is unknown and the bottom bounced energy can be detected.

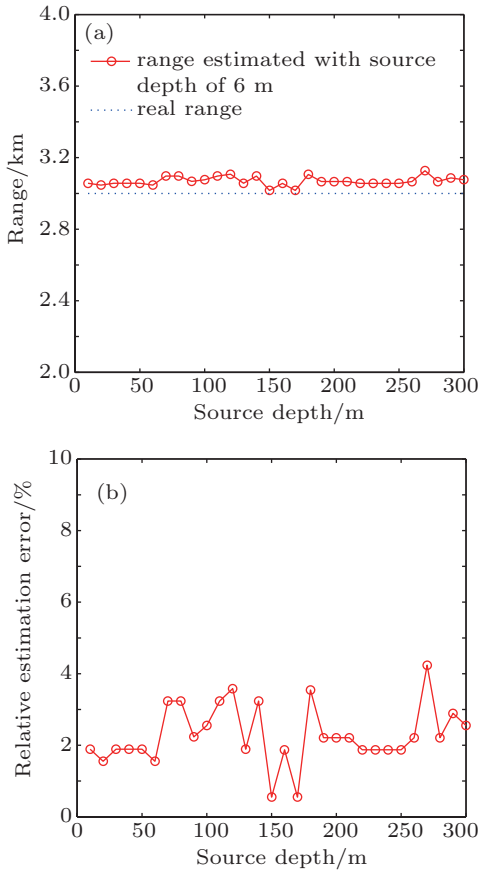


Fig. 11. (color online) (a) Ranges estimated and (b) relative estimation error versus source depth.

6. Summary

In this paper, low-frequency towed horizontal line array recordings are presented at a close range (< 18 km). Passing of a source ship and a tow ship is involved during the Northwest Pacific Acoustic Experiment in 2015. Broadband conventional beamforming is performed to the ship noise recorded on the array. A bearing-splitting phenomenon in the direct zone is observed, which might be misjudged as two different targets easily.

To explain the phenomenon, the ray theory is introduced. In terms of ray theory, sound field in the direct zone is mainly contributed by direct and bottom bounced paths. From the beam intensity equation, the bearing splitting is caused by the two groups of rays with significantly different arrival angles. Numerical simulations are performed and compared with experimental results. In both cases the bearings split into two parts. The one corresponding to the direct path is clearly visible within 3 km. It has a higher bearing-rate and is almost equal to the true bearing. The other one corresponding to the bottom bounced paths is evident during the observed voyage. It has a lower bearing-rate and is biased toward the broadside.

Finally, near-surface source ranges are estimated as an application of the split bearings in DZ. In deep water, the esti-

mated near-surface source ranges are related to source/receiver depths and arrival angles. For the near-surface source, as the depths of a surface ship and a towed horizontal line array are always known and the arrival angles could be obtained by the split bearings, source ranges can be estimated within an acceptable error. For the underwater source within several hundred meters in depth, the ranges could also be estimated by the split bearings even though the source depth is unknown, which is based on the poor sensitivity between range and source depth. Therefore, the source–receiver range could be estimated with an average error of less than 3% by taking an underwater source as a near-surface source.

Acknowledgement

The authors thank all of the participants from the State Key Laboratory of Acoustics in the 2015 Northwest Pacific Acoustic experiment.

References

[1] Heaney K D, Campbell R L and Murray J J, *et al.* 2013 *J. Acoust. Soc. Am.* **134** 3230
[2] Buckingham M J 1984 *IEE Proc.* **131** 298
[3] Yang T C 2003 *J. Acoust. Soc. Am.* **113** 1342
[4] Ma Y L, Liu M A, Zhang Z B, *et al.* 2003 *Chin. J. Acoust.* **22** 1
[5] Bucker H P 1976 *J. Acoust. Soc. Am.* **59** 368
[6] Thode A M 2000 *J. Acoust. Soc. Am.* **108** 1582
[7] Zhou S H, Qi Y B and Ren Y 2014 *Sci. China-Phys. Mech. Astron.* **57** 225
[8] Evan K W and David P K 1997 *J. Acoust. Soc. Am.* **102** 2645
[9] Duan R, Yang K D, Ma Y L, *et al.* 2014 *J. Acoust. Soc. Am.* **136** EL159
[10] Wu J N, Zhou S H and Zhang Y 2016 *Sci. China-Phys. Mech. Astron.* **46** 094311 (in Chinese)
[11] Wu J N, Zhou S H and Zhang Y 2015 *Technical Acoustics* **34** 267 (in Chinese)
[12] Jenson F B, K W A and Porter M B, *et al.* 1994 *Computational Ocean Acoustics* (New York: AIP Press) pp. 155–159
[13] Liu B S and Lei J Y 2009 *Principle of Acoustics in Water* (Harbin: Harbin Engineering University Press) (in Chinese)
[14] Michael B P 2011 *The BELLHOP Manual and User's Guide: PRELIMINARY DRAFT, Heat, Light, and Sound Research* (CA: Inc. La Jolla)